

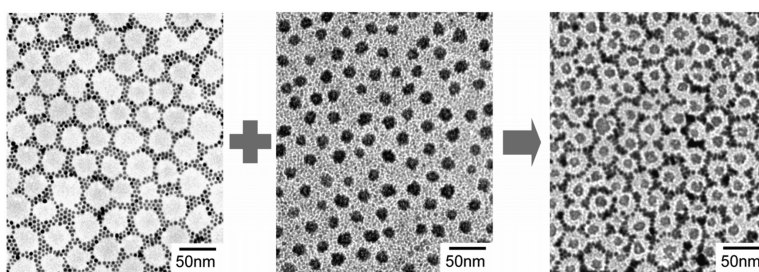
Communication

## Directed Self-Assembly of Two Kinds of Nanoparticles Utilizing Monolayer Films of Diblock Copolymer Micelles

Byeong-Hyeok Sohn, Jeong-Min Choi, Seong Il Yoo, Sang-Hyun Yun, Wang-Cheol Zin, Jin Chul Jung, Masayuki Kanehara, Takuji Hirata, and Toshiharu Teranishi

*J. Am. Chem. Soc.*, **2003**, 125 (21), 6368-6369 • DOI: 10.1021/ja035069w • Publication Date (Web): 01 May 2003

Downloaded from <http://pubs.acs.org> on March 28, 2009



### More About This Article

Additional resources and features associated with this article are available within the HTML version:

- Supporting Information
- Links to the 31 articles that cite this article, as of the time of this article download
- Access to high resolution figures
- Links to articles and content related to this article
- Copyright permission to reproduce figures and/or text from this article

[View the Full Text HTML](#)

## Directed Self-Assembly of Two Kinds of Nanoparticles Utilizing Monolayer Films of Diblock Copolymer Micelles

Byeong-Hyeok Sohn,<sup>\*,†</sup> Jeong-Min Choi,<sup>†</sup> Seong Il Yoo,<sup>†</sup> Sang-Hyun Yun,<sup>†</sup> Wang-Cheol Zin,<sup>†</sup> Jin Chul Jung,<sup>†</sup> Masayuki Kanehara,<sup>‡</sup> Takuji Hirata,<sup>‡</sup> and Toshiharu Teranishi<sup>‡,§</sup>

*Department of Materials Science and Engineering, Polymer Research Institute, Pohang University of Science and Technology, Pohang 790-784, Korea, School of Materials Science, Japan Advanced Institute of Science and Technology, and "Organization and Function", PRESTO, Japan Science and Technology Corporation, 1-1 Asahidai, Tatsunokuchi, Nomi, Ishikawa 923-1292, Japan*

Received March 9, 2003; E-mail: bhsohn@postech.ac.kr

Directed self-assembly of nanoparticles into specific structures can provide controlled fabrication of nanometer-sized building blocks with unique and useful electronic, optical, and magnetic properties.<sup>1–4</sup> In general, ligand- or polymer-stabilized nanoparticles can self-assemble into two-dimensional arrays.<sup>2,3,5,6</sup> On structured templates, two- or one-dimensional arrays of nanoparticles can be directed with particular arrangements.<sup>2,6–8</sup> For example, hexagonal arrays of nanoparticles on a monolayer of diblock copolymer micelles<sup>9</sup> and one-dimensional chains of nanoparticles on ridge-and-valley structured carbon<sup>10</sup> were demonstrated. Short-range self-assembled alloys of nanoparticles in two-dimensional arrays were also demonstrated.<sup>11</sup> In most cases of directed self-assembly, however, a single kind of nanoparticles was employed.<sup>1–10</sup>

In this Communication, we report a self-assembly of two kinds of nanoparticles simultaneously directed on a monolayer film of diblock copolymer micelles via physical and chemical arrangements. According to our knowledge, this work is the first attempt to direct two different types of nanoparticles on a structured template, as compared to all previous works that have focused on directing a single type of nanoparticle. Diblock copolymers composed of two different polymers form nanometer-sized micelles consisting of a soluble corona and an insoluble core in a selective solvent for one of the blocks.<sup>6</sup> These micelles can be coated onto substrates by spin coating to form a self-assembled nanostructure, which can serve as a structured template of nanoparticles.<sup>6–8,12</sup> We first incorporated gold nanoparticles physically around hexagonally ordered micelles of the monolayer film. Iron oxide nanoparticles were then synthesized chemically in the core area of the ordered micelles, resulting in iron oxide nanoparticles surrounded by gold nanoparticles.

For a monolayer film of diblock copolymer micelles, polystyrene-*block*-poly(4-vinylpyridine), PS-PVP ( $M_n^{PS} = 21.4$  kg/mol,  $M_n^{PVP} = 20.7$  kg/mol, polydispersity index = 1.13) was dissolved in toluene at 70 °C and cooled to room temperature to yield a 0.5 wt % micellar solution. Because toluene is a selective solvent for the PS block, spherical micelles of a PS corona and a PVP core were formed at this concentration. In the solution of PS-PVP micelles, we added 1.2 wt % dodecanethiol-protected gold nanoparticles (5.4 nm in diameter), which were synthesized and size-controlled as described elsewhere.<sup>13</sup> A monolayer film of PS-PVP micelles with gold nanoparticles was then fabricated simply by spin coating at 2000 rpm from the toluene solution on silicon wafers or freshly cleaved mica (ca. 1.5 cm × 1.5 cm), as described in our previous report.<sup>12</sup> After residual solvents were evacuated, the film was separated from the mica substrate by floating on water.<sup>12</sup> The film

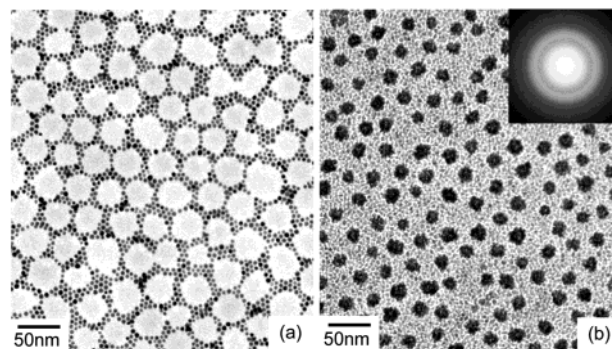


**Figure 1.** TEM images: (a) gold nanoparticles located around the micelles; (b) array of iron oxide nanoparticles synthesized with oxygen plasma treatment. The inset is a selected-area electron diffraction pattern of iron oxide nanoparticles.

was transferred to a copper grid for transmission electron microscopy (TEM). As shown in Figure 1a, gold nanoparticles were decorated around the micelles having a short-range hexagonal order, which were indirectly visualized as the region surrounded by gold nanoparticles. In addition, gold nanoparticles themselves were organized with a regular spacing due to dodecanethiol groups on the particle surface, resulting in a hierarchical self-assembly of nanoparticles in copolymer micelles. In the TEM image of the PVP core loaded with FeCl<sub>3</sub> (Supporting Information Figure S1), the bright PS gap was visible between the gray PVP core and gold nanoparticles, implying that gold nanoparticles were not located in the entire PS coronas. Alkylthiol-protected gold nanoparticles cannot be miscible with either polar PVP blocks or aromatic PS blocks. Moreover, gold nanoparticles were much smaller than PS-PVP micelles. Thus, they could be physically arrested between the micelles with possible overlapping with PS coronas, presumably due to capillary force generated between the micelles during the formation of micellar monolayers. Although the number of gold nanoparticles encircling each micelle was fluctuated in the film, the total amount around the micelles was controllable with their concentration in the solution. Thus, we were able to direct gold nanoparticles around the micelles with a hierarchical order in self-assemblies of nanoparticles and copolymer micelles.

Because a variety of metal salts can be selectively coordinated to the PVP block,<sup>6</sup> FeCl<sub>3</sub> was dissolved in a 0.5 wt % toluene solution of PS-PVP micelles (molar ratio of FeCl<sub>3</sub>/vinylpyridine = 0.3) without gold nanoparticles. From this solution, we spin-coated a monolayer film of PS-PVP micelles containing FeCl<sub>3</sub> in the core, which was confirmed by dark PVP cores, due to selectively loaded FeCl<sub>3</sub>, in the TEM image (Supporting Information Figure S2). To synthesize iron oxide nanoparticles, a film of hexagonally

<sup>†</sup> Pohang University of Science and Technology.

<sup>‡</sup> Japan Advanced Institute of Science and Technology.

<sup>§</sup> Japan Science and Technology Corp.

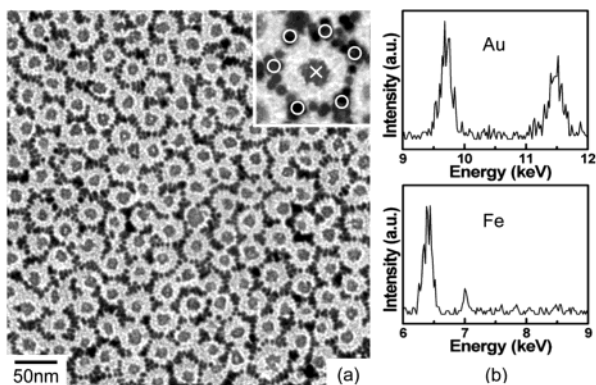


**Figure 2.** (a) TEM image of an array of iron oxide nanoparticles surrounded by gold nanoparticles; (b) EDX spectra on gold and iron nanoparticles marked by circles and a cross in the enlarged TEM image, respectively.

ordered PS-PVP micelles containing  $\text{FeCl}_3$  was treated with oxygen plasma ( $110 \text{ W}$ ,  $2.0 \times 10^{-2} \text{ Torr}$ ) for  $10 \text{ min}$ ,<sup>14</sup> resulting in oxidation of  $\text{FeCl}_3$  and removal of organic PS-PVP micelles. The plasma treatment was performed with the film on silicon wafers or TEM-grid-sized silicon substrates having a silicon nitride membrane window for TEM analysis.<sup>8,15</sup> As shown in Figure 1b, an array of iron oxide nanoparticles was fabricated with the preservation of a short-range hexagonal order of the micelles, implying that metal salts in each core were oxidized to a single nanoparticle.<sup>14</sup> The diameter of iron oxide nanoparticles (ca.  $16 \text{ nm}$ ) was smaller than that of the PVP core (ca.  $23 \text{ nm}$ ), possibly because of densification by removal of PVP blocks as well as a dose of  $\text{FeCl}_3$  to vinylpyridine ( $0.3$  molar ratio). In atomic force microscopy (AFM) and field-emission scanning electron microscopy (FE-SEM) images of iron oxide nanoparticles on silicon wafers, each iron oxide nanoparticle appeared as a hemisphere ca.  $12 \text{ nm}$  in height (Supporting Information Figure S3). The selected-area electron diffraction pattern shown in the inset of Figure 1b verified the iron oxide structure as  $\gamma\text{-Fe}_2\text{O}_3$ , which is a magnetic material. In addition, X-ray photoelectron spectroscopy (XPS) results confirmed complete removal of PS-PVP copolymers by the disappearance of carbon photoelectrons. Thus, we were able to fabricate iron oxide nanoparticles with a specific arrangement by chemical synthesis executed on a monolayer of PS-PVP micelles.

To construct a self-assembled structure of both gold and iron oxide nanoparticles concurrently on a monolayer film of PS-PVP micelles, dodecanethiol-protected gold nanoparticles were added to the toluene solution of PS-PVP micelles containing  $\text{FeCl}_3$  with the same concentration as before. From this solution, we again spin-coated a monolayer film of hexagonally ordered PS-PVP micelles containing gold nanoparticles around the micelles and  $\text{FeCl}_3$  in the core, which was confirmed by TEM (Supporting Information Figure S1). The monolayer film was then treated with oxygen plasma to generate iron oxide nanoparticles. Figure 2a shows a TEM image of hexagonally ordered iron oxide nanoparticles that were surrounded by gold nanoparticles, that is, a combined image of Figure 1a and b. Gold nanoparticles did not directly contact with iron oxide nanoparticles because of the gap between gold nanoparticles and the PVP core containing  $\text{FeCl}_3$ , and the size reduction of core areas after plasma treatment. Figure 2b shows energy-dispersive X-ray

(EDX) spectra on gold and iron nanoparticles marked by circles and a cross in the enlarged TEM image, respectively. The EDX results of  $9.7 \text{ keV}$  ( $\text{Au L}\alpha$ ),  $11.4 \text{ keV}$  ( $\text{Au L}\beta$ ),  $6.4 \text{ keV}$  ( $\text{Fe K}\alpha$ ), and  $7.0 \text{ keV}$  ( $\text{Fe K}\beta$ ) also confirmed the location of gold and iron atoms. In XPS spectra, no carbon photoelectrons were observed, implying that not only PS-PVP copolymers but also dodecanethiol on gold nanoparticles were completely removed by oxygen plasma. Elimination of the protecting ligands induced the aggregation of gold nanoparticles as shown in Figure 2a, which had been arranged with an equal gap. At the condition of oxygen plasma that we used, however, oxidation of gold nanoparticles did not occur,<sup>16</sup> according to the XPS result, in which two characteristic spectra of Au-4f photoelectrons of pure gold were observed at  $84.0$  and  $87.7 \text{ eV}$ . Therefore, we were able to produce a directed self-assembly of magnetic iron oxide nanoparticles in a short-range hexagonal array, which were encircled by metallic gold nanoparticles.

In conclusion, we successfully demonstrated a directed self-assembly of two different kinds of nanoparticles on a block copolymer micellar template. Controlling more than a single type of nanoparticles in specific positions can provide an opportunity to utilize unique properties of each type of nanoparticle. Thus, the methodology demonstrated in this study can be a good example of how different types of functional nanometer-sized building blocks can be organized in specific arrangements by physical and chemical self-assembling procedures on structured templates.

**Acknowledgment.** This work was supported by Korea Research Foundation Grant (KRF-2002-003-D00097). This work was also supported in part by PRESTO, JST and by a Grant-in-Aid for Scientific Research on Encouragement Research (A) (No. 13740392) from the Ministry of Education, Culture, Sports, Science, and Technology, Japan (T.T.).

**Supporting Information Available:** Figures S1–S3 (PDF). This material is available free of charge via the Internet at <http://pubs.acs.org>.

## References

- (1) Alivisatos, A. P. *Science* **1996**, *271*, 933.
- (2) Murray, C. B.; Kagan, C. R.; Bawendi, M. G. *Annu. Rev. Mater. Sci.* **2000**, *30*, 545.
- (3) Sun, S.; Murray, C. B.; Weller, D.; Folks, L.; Moser, A. *Science* **2000**, *287*, 1989.
- (4) Lin, Y.; Skaff, H.; Emrick, T.; Dinsmore, A. D.; Russell, T. P. *Science* **2003**, *299*, 226.
- (5) Teranishi, T.; Haga, M.; Shiozawa, Y.; Miyake, M. *J. Am. Chem. Soc.* **2000**, *122*, 4237.
- (6) Förster, S.; Antonietti, M. *Adv. Mater.* **1998**, *10*, 195.
- (7) Cox, J. K.; Eisenberg, A.; Lennox, R. B. *Curr. Opin. Colloid Interface Sci.* **1999**, *4*, 52.
- (8) Lopes, W. A.; Jaeger, H. M. *Nature* **2001**, *414*, 735.
- (9) Spatz, J. P.; Roescher, A.; Möller, M. *Adv. Mater.* **1996**, *8*, 337.
- (10) Teranishi, T.; Sugawara, A.; Shimizu, T.; Miyake, M. *J. Am. Chem. Soc.* **2002**, *124*, 4210.
- (11) Kiely, C. J.; Fink, J.; Zheng, J. G.; Brust, M.; Bethell, D.; Schiffrin, D. J. *Adv. Mater.* **2000**, *12*, 640.
- (12) Sohn, B. H.; Yoo, S. I.; Seo, B. W.; Yun, S. H.; Park, S. M. *J. Am. Chem. Soc.* **2001**, *123*, 12734.
- (13) Teranishi, T.; Hasegawa, S.; Shimizu, T.; Miyake, M. *Adv. Mater.* **2001**, *13*, 1699.
- (14) Spatz, J. P.; Mössmer, S.; Hartmann, C.; Möller, M.; Herzog, T.; Krieger, M.; Boyen, H.-G.; Ziemann, P.; Kabis, B. *Langmuir* **2000**, *16*, 407.
- (15) Boontongkong, Y.; Cohen, R. E. *Macromolecules* **2002**, *35*, 3647.
- (16) Boyen, H.-G.; Kästle, G.; Weigl, F.; Koslowski, B.; Dietrich, C.; Ziemann, P.; Spatz, J. P.; Riethmüller, S.; Hartmann, C.; Möller, M.; Schmid, G.; Garnier, M. G.; Oelhafen, P. *Science* **2002**, *297*, 1533.

JA035069W